Desalination and Water Treatment
www.deswater.com

doi: 10.1080/19443994.2015.1083888

57 (2016) 16733–16744
August

Taylor & Francis
Taylor & Francis Group

Reverse osmosis membranes prepared by interfacial polymerization in n-heptane containing different co-solvents

A.S. AL-Hobaib[a,*], M.S. Alsuhybani[a], Kh.M. AL-Sheetan[a], Mohammed Rafi Shaik[b]

[a]*Institute of Atomic Energy Research, King Abdulaziz City for Science and Technology (KACST), P.O. Box 6086, Riyadh 11442, Saudi Arabia, Tel. +966 114813675; Fax: +966 114813646; email: ahobaib@kacst.edu.sa (A.S. AL-Hobaib), Tel. +966 114813675; emails: sohybani@kacst.edu.sa (M.S. Alsuhybani), ksheetan@kacst.edu.sa (Kh.M. AL-Sheetan)*
[b]*Department of Chemistry, College of Sciences, King Saud University (KSU), P.O. Box 2455, Riyadh 11451, Saudi Arabia, Tel. +966 114670439; email: rafiskm@gmail.com*

Received 9 December 2014; Accepted 11 August 2015

ABSTRACT

The objective of this work was to develop a suitable and highly efficient reverse osmosis membrane incorporating a co-solvent system. A polyamide thin-film composite membrane has been prepared by interfacial polymerization in n-heptane using diethyl ether and ethyl acetate as co-solvents at various concentrations. Heptane has a molecule of larger C–C chain than that of traditionally used hexane. Heptane was selected in order to study its effect on the morphology of the prepared membrane as well as on salt rejection ability and flux volume. Heptane appeared to produce an improved morphology, salt rejection ability, and flux volume, compared to hexane. To the best of our knowledge, this is the first attempt to prepare and characterize TFC RO membrane in n-heptane mixed with co-solvent. The membranes were characterized using microscopy, spectroscopy, and contact angle measurement techniques. From surface spectroscopic analyses, the addition of co-solvents led to a decrease in the roughness properties of the membranes. The synthesized polyamide membranes consist of large and ordinal ridge-and-valley formations. The salt rejection and water permeate flux were well controlled by the categories and amounts of co-solvents that were added. Thermal gravimetric analysis results indicated that all of the membranes exhibited high thermal stability with degradation temperatures of about 481 ± 2˚C. The high stability of the membranes was attributed to the sulfonic groups on the polymer chains. The contact angle also increased with an increasing co-solvent concentration. The performance characteristics of the membranes were evaluated by measuring the flux and rejection of isopropyl alcohol, NaCl, and $MgCl_2$ solutions. The rate of flux was proportional to the co-solvent concentration (i.e. flux increases with an increasing concentration), whereas the salt rejection properties were constantly high. Membranes formed with diethyl ether showed the highest salt rejection. Based on these data, membranes prepared using diethyl ether or ethyl acetate as a co-solvent in a non-polar heptane medium performed efficiently and exhibited high salt rejection characteristics with large flux values. These membranes represent promising candidates for freshwater desalination and removal of organic impurities.

Keywords: Interfacial polymerization; Modified reverse osmosis membrane; Desalination; Co-solvent

*Corresponding author.

1. Introduction

Most of the water used by humans is collected from rivers, lakes, canals, ponds, and underground aquifers since ancient times [1]. These freshwater sources are being depleted at an increasing rate by population growth, industrialization, modernization, and climate change. Industrial and agricultural wastes contaminate lakes, canals, and rivers and ultimately leach into underground water sources. These effluents contain a wide range of dangerous contaminants, such as metals, dyes, pesticides, fertilizers, and biological agents, which are toxic to humans and therefore unsuitable for human consumption [2,3]. For this reason, significant research efforts have been directed towards developing new technologies and processes for the production of fresh drinking water.

New and innovative techniques for the desalination of ocean water and the purification of industrial effluents are being continuously developed. Thus, filtration of ocean water or contaminated industrial effluents through membranes, reverse osmosis (RO), and nanofiltration (NF) membranes with good desalination performances and high permeate flux has been developed [4–11].

RO membranes exhibit a very high level of rejection towards inorganic solutes such as monovalent ions and hardness components (e.g. calcium and magnesium), and organic materials such as trihalo-methane precursors, pesticides, and deodorants [12]. RO membranes are generally composed of three layers, including (a) unwoven polyester, (b) polysulfone or polyethersulfone, and (c) polyamide or polyetherimide. The polyamide membranes used in RO membranes are prepared by an interfacial polymerization reaction between 1,3-phenylenediamine (MPD) in the water phase and 1,3,5-benzenetricarbonyl trichloride (TMC) in the non-polar organic phase. FT-30 is an industrially produced RO membrane, which has a high salt rejection of more than 99% and a flux greater than 1 m^3/m^2d for 2,000 ppm NaCl at 1.55 MPa [13]. To assess the PS support membrane, a dead-end test system was used for measuring pure water permeate flux and molecular weight cut-off (MWCO). The MWCO of a membrane is generally defined as the molecular weight of a solute at which above 90% of the solute is retained.

Kamada et al. developed a series of polyamide-based RO membranes with controlled surface morphology via the interfacial polymerization of MPD with TMC on a polysulfone ultrafiltration support using hexane as a non-polar organic reaction solvent [14]. The addition of a co-solvent to the organic phase such as acetone, ethyl acetate, or diethyl ether was also investigated by Kamada to control both the surface morphology and the polyamide network matrix. Optimum results of 99% (NaCl rejection and a permeate flux of more than 1.8 m^3/m^2d at 1.5 MPa) were achieved when 3 wt% ethyl acetate was used. Notably, the permeate flux rate was threefold higher than that of the corresponding RO membrane prepared without any co-solvent. Kong et al. investigated the use of acetone (2 wt%) as a synergistic co-solvent in the hexane phase to control the polymerization reaction as well as modifying the membrane network matrix [15]. This membrane showed selective molecular sieving properties with a preference for small molecules over larger molecules. Furthermore, the addition of a larger amount of the acetone co-solvent to the hexane solution led to an increase in the pore size and water flux properties of the resulting membrane. RO membranes produced using 2 wt% acetone as a co-solvent showed a rejection of more than 99.4% and high water transport at a rate of more than 1×10^{-11} m^3/m^2 Pa s, which was more than fourfold higher than that obtained from the RO membrane prepared without acetone. Polyamide membranes with controllable, thin dense layers, and effective nanopores were also fabricated by Kong et al. [16] by the interfacial polymerization of MPD with TMC using acetone as a co-solvent with hexane as the non-polar organic phase, and the resulting membranes exhibited high water flux and salt rejection properties. Addition of 2 wt% acetone as a co-solvent in this case led to an approximate fourfold increase in water flux with no loss of salt rejection compared with the corresponding membrane prepared without acetone. The incorporation of a co-solvent to the organic phase during the interfacial polymerization of MPD with TMC induces structural and morphological changes in the resulting RO membranes [17–19]. Yu et al. developed a thin-film composite (TFC) RO polyamide–urethane membrane for sea water desalination via interfacial polymerization of MPD and 5-chloroformyloxyisophthaloyl chloride (CFIC) microporous polysulfone supporting membrane support using hexane as a organic reaction solvent. The water flux of the developed membrane increases from about 35 l/m^2 h to around 42 l/m^2 h and the salt rejection is constantly above 99.4% [20]. Zou et al. synthesized RO thin-film composite membrane via novel approach of interfacial polymerization of MPD, trimethylamine (TEA), and camphor sulfonic acid on polysulphone supports. The membrane performance of water flux is 33.35 l/m^2 h and salt rejection is above 98.5%, and it is varied greatly with the contact time [21].

This was the primary high-performance polyamide membrane manufactured using co-solvent-assisted interfacial polymerization (CAIP). This attractive and

encouraging approach opened up new ways to further improve polyamide membranes with the addition of co-solvents into the organic phase. We selected two types of co-solvents, diethyl ether and ethyl acetate, to use, which result in high water flux and salt rejection. In the present study, heptane has a molecule of larger C–C chain than that of traditionally used organic solvents. Heptane appeared to produce an improved morphology, salt rejection ability, and flux volume, compared to other organic solvents.

2. Experimental

2.1. Materials and methods

2.1.1. Materials

All of the chemicals and reagents used in this study were purchased at the highest purity grades available. Polyamide composite membranes were prepared on an ultrafiltration polysulfone (PS-20, The microporous polysulphone supporting film with (MWCO) molecular weight cut-off 20 k Da and, Water Permeate Flux 1,000 LMH/bar, Sepro) 1,3-phenylenediamine (MPD, >99%, Sigma, St. Louis, MO, USA) with 1,3,5-benzenetricarbonyl trichloride (TMC, >98%, Sigma). A detailed description of the method used for the preparation the polymers is provided below.

2.1.2. Preparation of membrane

PS was immersed in an aqueous solution of 2 wt% MPD for 2 min. The excess MPD solution was then removed by pressing the commercially available polysulfone product support (PS-20) PS material under a rubber roller. The freshly pressed material was then immersed in a 0.1 wt% solution of TMC in heptane

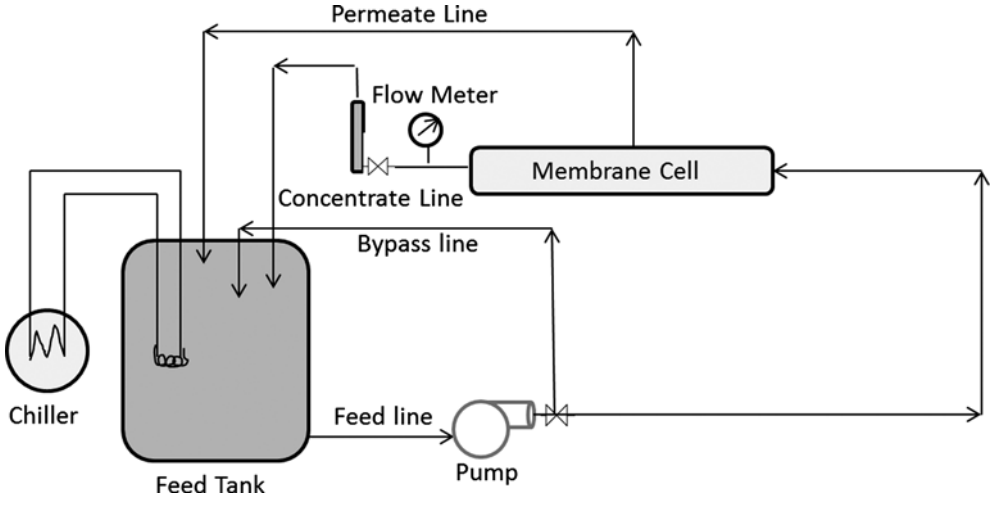

Fig. 1. Schematic illustration of forward cross-flow filtration system.

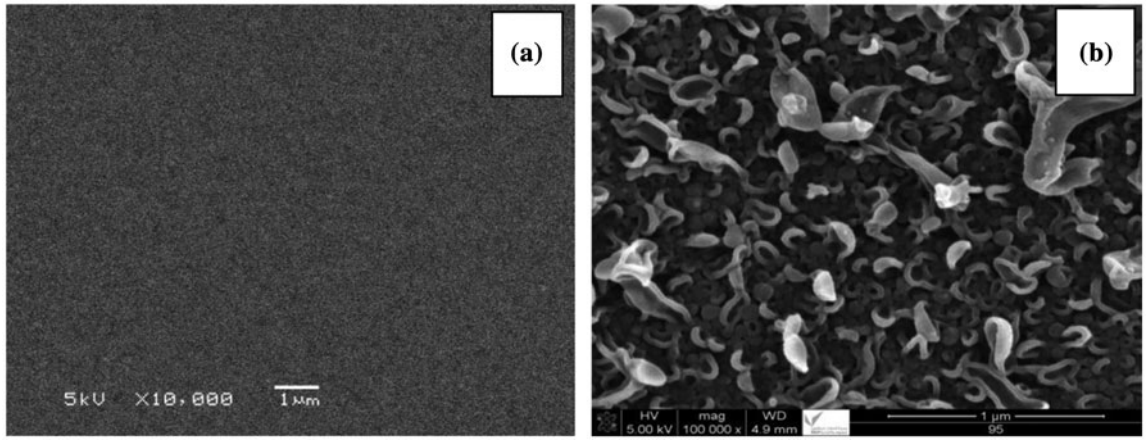

Fig. 2. SEM images: (a) PS membrane and (b) TFC reference membrane.

(99%, Sigma) for 1 min containing different quantities of co-solvent (0.5, 1, 2, 3, and 5 wt%). The product was then rinsed with 0.2 wt% Na_2CO_3 (>99%, Scharlau,), washed with DI water, and then stored in a refrigerator at about 4˚C in DI water prior to being used. Ethyl acetate (>99%, Sigma) and diethyl ether (>99%, Sigma) were investigated as co-solvents in the current study [15,16]. In this way, a total of 11

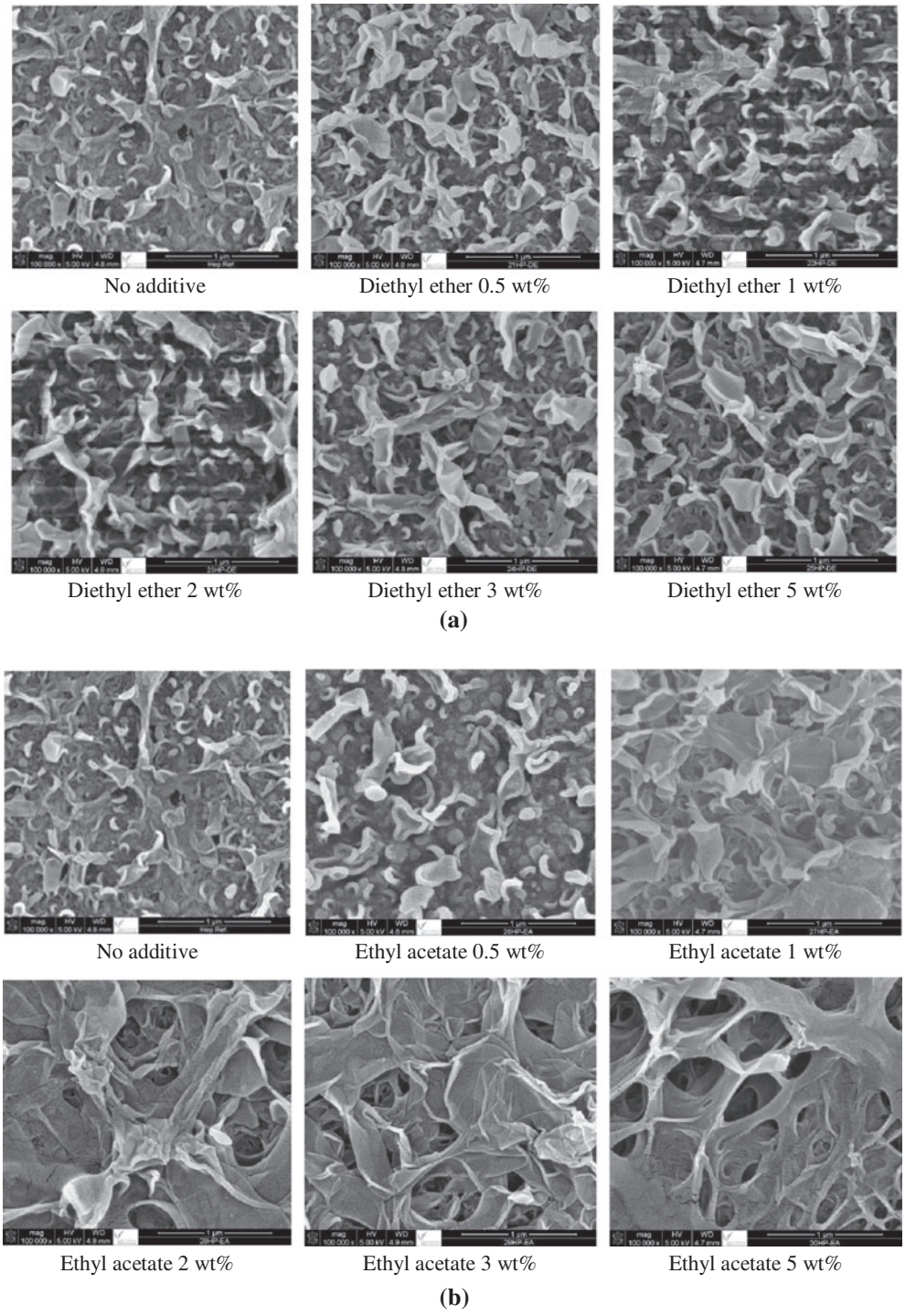

Fig. 3. SEM images showing the effect of the added co-solvent (a) diethyl ether and (b) ethyl acetate on the morphology of the resulting membrane.

different polyamide membranes were fabricated in this study. All of these membranes were fully characterized using a range of different analytical techniques to evaluate their performance characteristics with respect to their salt-rejecting ability and water permeate flux volume.

2.1.3. Characterization and instrumentation

The morphological and microstructural characteristics of the composite membranes were examined by scanning electron microscopy (SEM, FEI Nova-Nano SEM-600, Netherlands). Atomic force microscopy (AFM) was used to analyze the surface morphology and roughness of the membranes. AFM images were recorded on a nanosurf scanning probe-optical microscope (Bruker Corporation). Small squares of the membranes (approximately 1 cm^2) were cut out and glued on to the surface of a glass substrate for analysis. The thermal stability properties of the membranes with different co-solvent concentrations were characterized by thermogravimetric analysis (TGA) using a Pyris 1 TGA system (PerkinElmer, USA). The TGA experiments were heated from ambient temperature to 800°C at a heating rate of 10°C/min and a nitrogen gas flow of 20 ml/min using a ceramic pan. FT-IR spectroscopy was conducted with an attenuated total reflection (ATR) plate (Perkin Elmer) to identify the chemical compositions of the membrane. The polyamide layer surfaces of the membrane samples were placed face-down on the crystal surface. The FT-IR-ATR spectra were measured at frequencies in the range of 4,000–600 cm^{-1} at a resolution of 4 cm^{-1}. Contact angle analysis was performed using a Ramé-Hart Model 250 Standard Goniometer/Tensiometer with drop image advanced software (Ramé-Hart Instrument Co., Succasunna, NJ, USA). A water droplet was placed on a dry flat homogeneous membrane surface, and the contact angle between the water droplet and the membrane was measured until no further change was observed. The average contact angle for distilled water was determined following a series of eight measurements for each of the different membrane surfaces. The performance characteristics of the prepared membranes were analyzed using a cross-flow system (CF042SS316 Cell, Sterlitech Corp., USA). The valid membrane area in this system was 42 cm^2. The feed water temperature was set at 25°C with a pH value in the range of 6–7, and a 2,000 ppm NaCl feed stream at a flow rate of 1 gallon per minute (gpm). The filtration was carried out at the pressure of 225 psi. All of the water flux and salt rejection measurements were taken after 30 min of the water filtration experiments to ensure that the system had reached a steady state. A

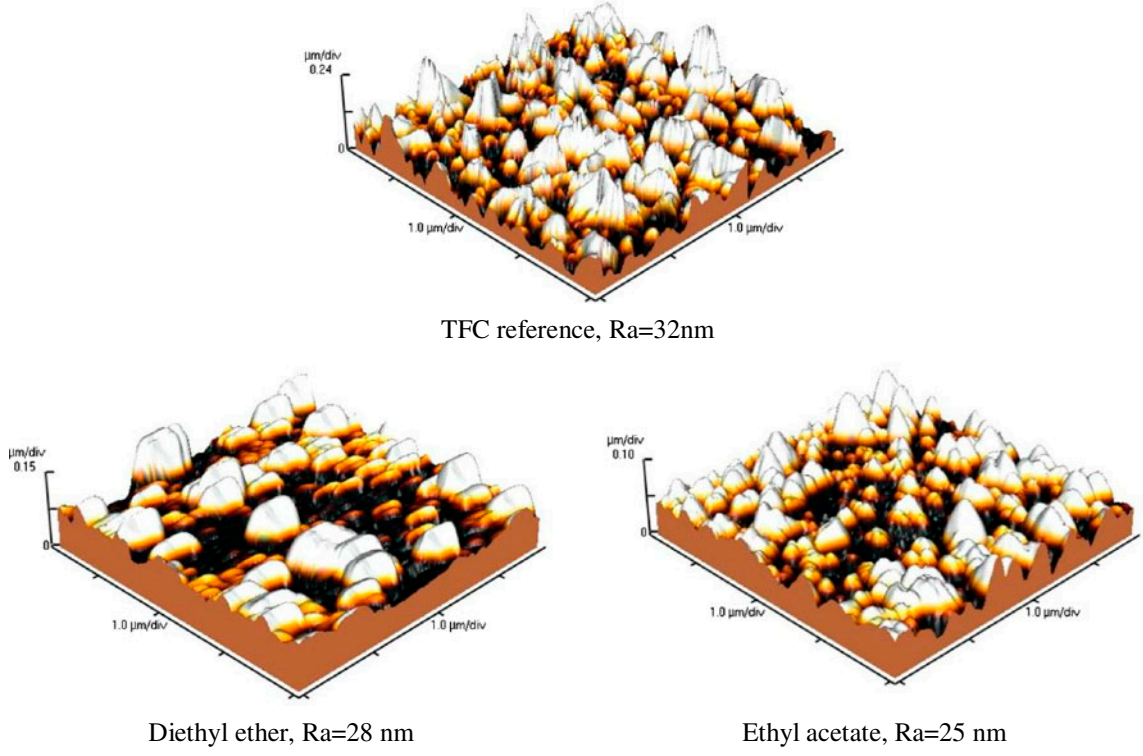

Fig. 4. AFM images of the different membranes.

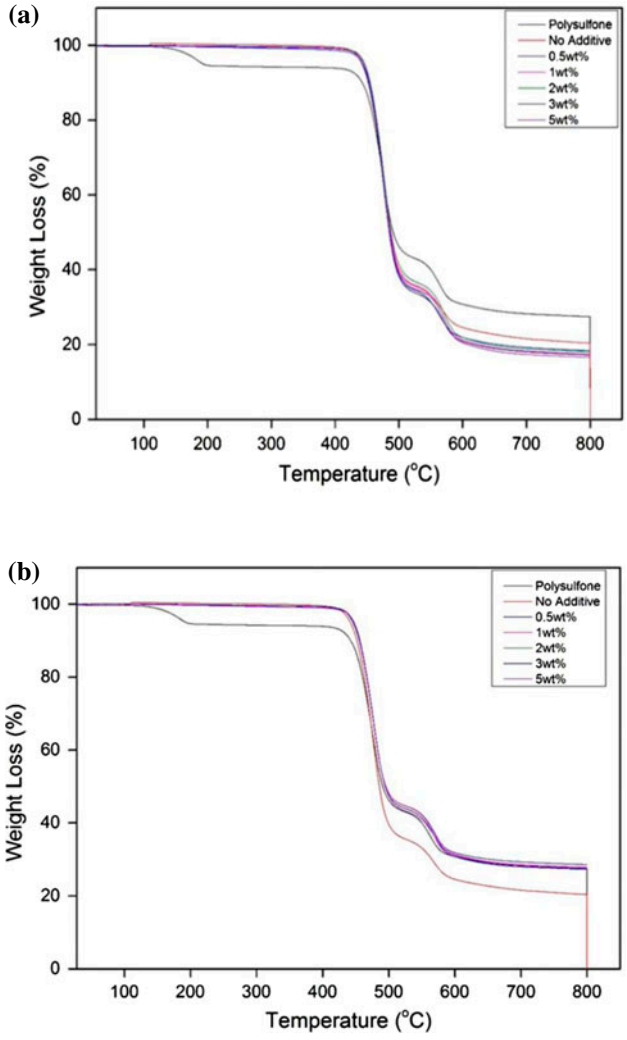

Fig. 5. TGA results obtained for membranes containing polyamide and polysulfone with different concentrations of a co-solvent: (a) diethyl ether and (b) ethyl acetate.

schematic diagram of the cross-flow filtration system is shown in Fig. 1.

The flux was calculated using the following equation [20]:

$$J = \frac{V_p}{A \times t} \quad (1)$$

where J is the water flux (L/m^2 h), V_p is the permeate volume (L), A is the membrane area (m^2), and t is the treatment time (h). The salt rejection (R) was calculated using the following equation:

$$R = \left(1 - \frac{C_p}{C_f}\right) \times 100 \quad (2)$$

where C_p and C_f are the salt concentrations of the permeate and the feed, respectively.

3. Results and discussion

3.1. SEM analysis

SEM images of the polysulfone (PS) base and TFC reference materials are shown in Fig. 2(a) and (b), respectively. These images show that the surfaces of these membranes were smooth and homogeneous.

SEM images of membranes after addition of co-solvents show that the co-solvent concentration has a significant effect on the morphology of the membranes (Fig. 3(a) and (b)). The current results were in agreement with those reported by other researchers working in this field [17–19]. The polyamide layer is a non-porous dense layer. The surface morphology of the synthesized polyamide membrane without co-solvent addition displayed the ordinal ridge-and-valley structures. The morphology increased the surface area and surface roughness of the polyamide membrane, which

Table 1
TGA values obtained from the membranes of polyamide with polysulfone

Conc. (wt%)	Code	First high peak	Second high peak	Weight loss % at 800°C	Residual mass % at 800°C
0	Polysulfone	479.90	576.30	72.30	27.70
0	TFC-reference	483.11	581.89	79.23	20.77
0.5	Diethyl ether	481.76	581.38	79.33	20.67
	Ethyl acetate	483.64	582.62	79.27	20.73
1.0	Diethyl ether	481.7	581.43	78.13	21.87
	Ethyl acetate	484.15	587.8	79.89	20.11
2.0	Diethyl ether	481.74	580.87	79.19	20.81
	Ethyl acetate	482.28	582.44	79.46	20.54
3.0	Diethyl ether	480.95	579.53	78.97	21.03
	Ethyl acetate	481.7	583.89	78.73	21.27
5.0	Diethyl ether	485.16	583.83	78.44	21.56
	Ethyl acetate	482.2	580.81	77.93	22.07

was effective for water permeation flux and salt rejection. From the literature review, it should be well-known that with the addition of co-solvents in polyamide membrane displayed a ridge-and-valley structure with a height of several hundred nm. However, in contrast to Kamada's study, heptane was used as the non-polar organic phase in the current study instead of hexane.

3.2. Atomic force microscopy

AFM images of the membranes are shown in Fig. 4. The surfaces of the membranes had roughness values in the range of 25–32 nm. The surfaces of the membranes consisted of continuous ridges and valleys, and these results were therefore consistent with those reported by other researchers [17–19].

3.3. Thermogravimetric analysis

Fig. 5(a) and (b) shows the thermal degradation behaviors of the different membranes prepared using polyamide on a polysulfone platform with different concentrations of the co-solvents in the TMC layer. It is clear from the figure that the thermal decomposition of the PS and PA membranes involved two main

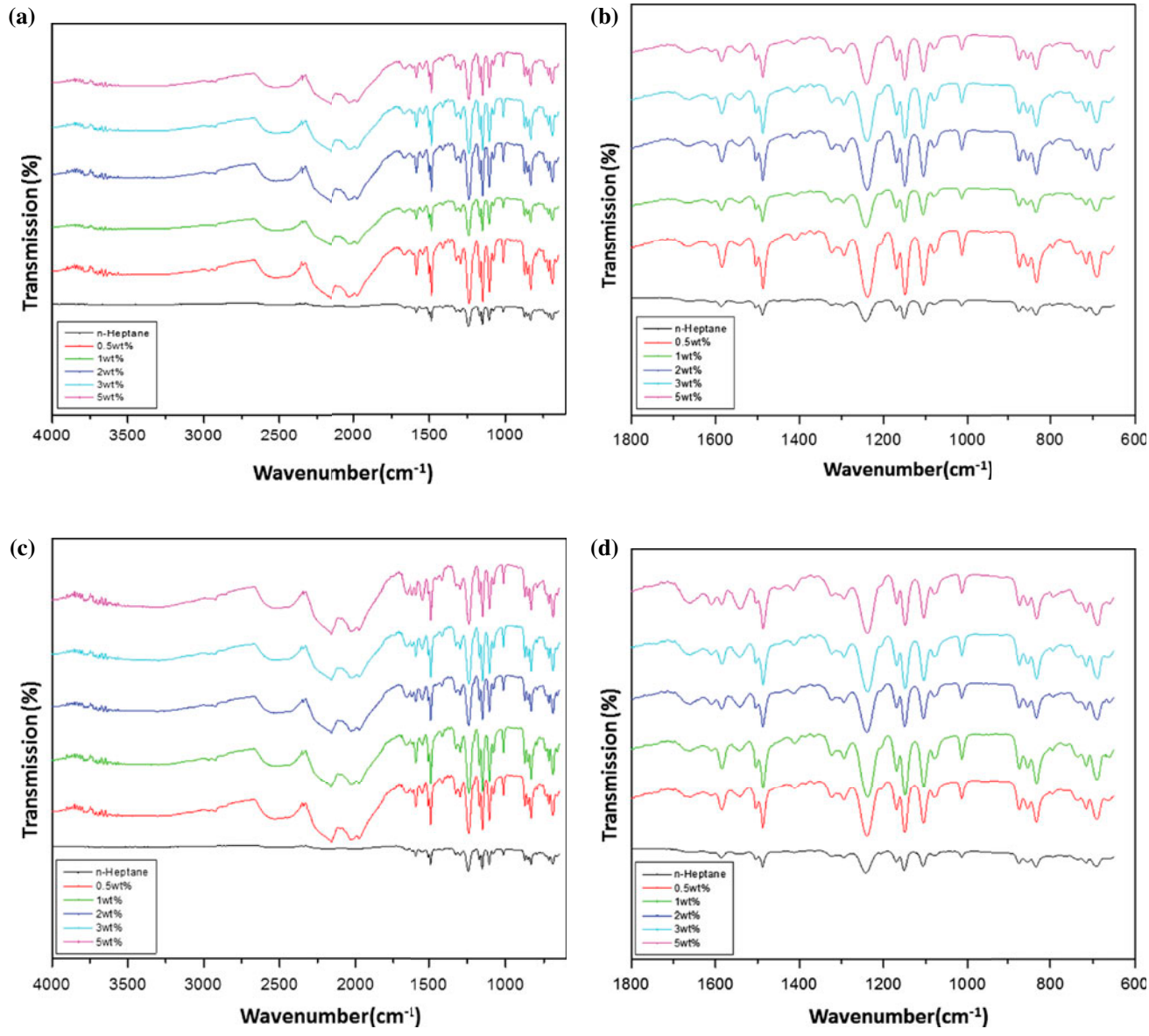

Fig. 6. ATR-FTIR spectra of membranes containing diethyl ether or ethyl acetate as a co-solvent: (a) heptane-diethyl ether, (b) heptane-diethyl ether, (c) heptane-ethyl acetate, and (d) heptane-ethyl acetate.

steps, with the first of these steps occurred at temperatures in the range of 400–500˚C, and the second degradation step occurred at temperatures in the range of 550–600˚C. These results are in good agreement with the results reported by other researchers [8,22,23]. Interestingly, however, a small degradation step was observed at temperatures in the range of 100–170˚C for PS, this was due to the release of physically absorbed water. This peak was observed in only PS and it was not observed in PA membrane because the peaks are caused by amide linkage, and sulfone base fracture of polyamide membrane structure is quite stable. Only when the temperature is rather high, the amide and sulfone will rupture. Data for the degradation peaks, weight loss, and residual mass derived from Fig. 5(a) and (b) of the different membranes formed in the presence of different quantities of the two co-solvents are shown in Table 1. These results indicate that all of the membranes prepared in the current study possess high thermal stability with degradation temperatures of about 481 ± 2˚C. This high level of stability could be attributed to the sulfonic acid groups on the polymer chains. These findings are consistent with those reported by other researchers working in this field [24]. However, the second degradation step around 580 ± 3˚C was caused by the occurrence of polymerization and cross-linking processes during the formation of the polyamide membrane [25]. Table 1 shows the residual weights of all of the samples at 800˚C. The residual weights were

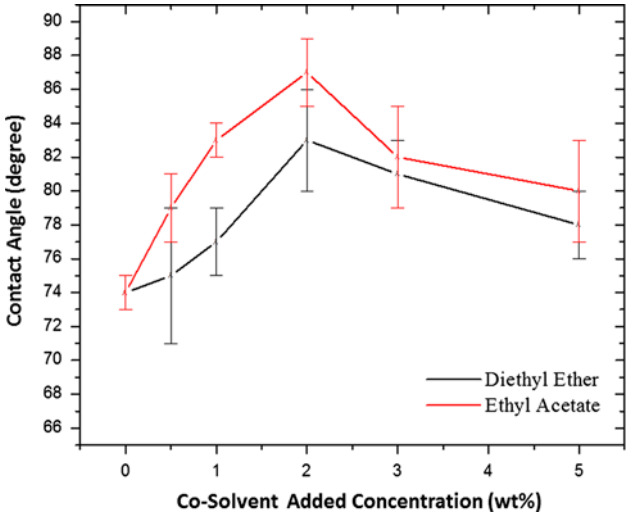

Fig. 7. Contact angles plotted against concentration of co-solvent.

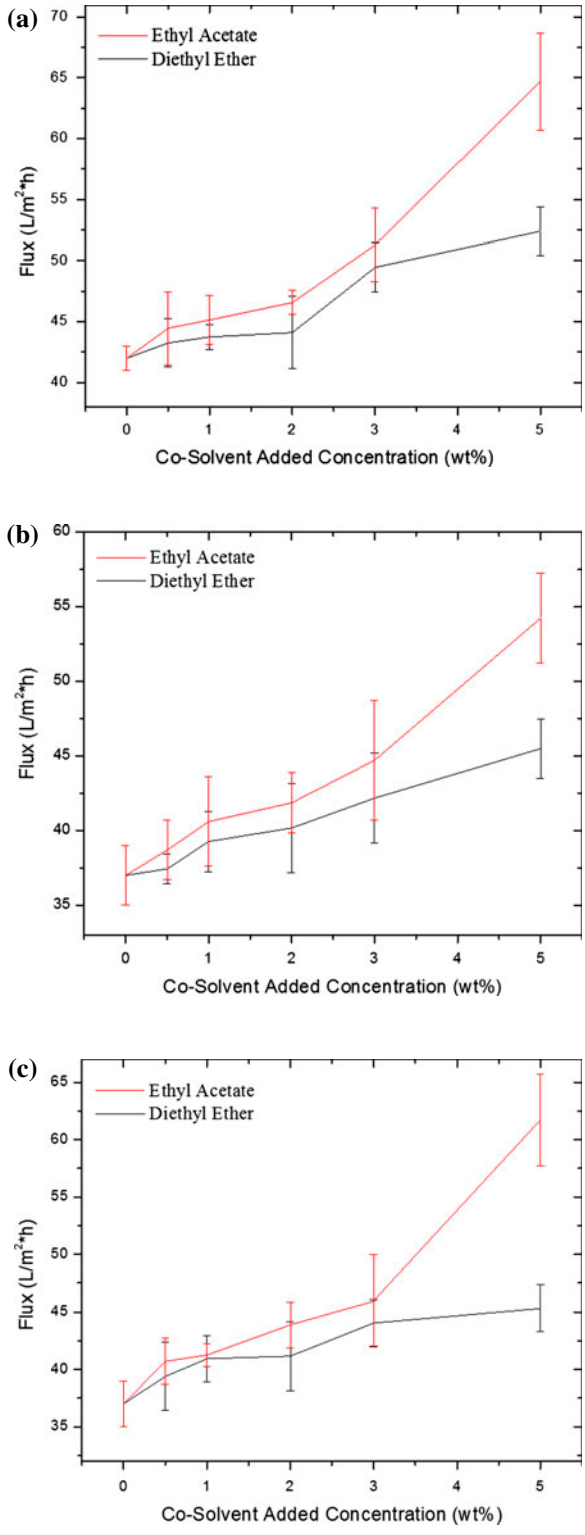

Fig. 8. Flux rates through membranes containing different co-solvents: (a) flux of IPA, (b) flux of NaCl, and (c) flux of MgCl2.

found to be 20–22.1% of the original sample weights depending on the concentration of co-solvent.

3.3.1. Attenuated total reflection Fourier transmission infrared spectroscopy

ATR-FTIR spectra under the absorbance mode for the polyamide layers that were synthesized with the addition of ethyl acetate and diethyl ether as co-solvents, ranging from 0.5 to 5 wt% in order to attain a quantitative amount of polyamide skin layer and amide bond content. FT-IR spectra of the membranes prepared using diethyl ether or ethyl acetate as a co-solvent were recorded in the range of 600–4,000 cm^{-1} (Fig. 6(a)–(d)). These spectra also show the effect of the co-solvent concentration, in that the transmission (%) of light decreased with an increasing co-solvent concentration. Furthermore, the absorption of light energy increased with an increasing co-solvent concentration, which was indicative of the formation of a thicker membrane layer. The signal attributed to the $–CH_2–$ groups at 780 cm^{-1} appeared to be influenced by the addition of ethyl acetate. Long-chain methyl rock (780) is noted on this ethyl acetate spectrum and a strong band appeared at about 1,752 cm^{-1} which is the characteristic of a C=O stretch, although a similar effect was not observed in the diethyl ether because of C–O stretch in the region 1,300–1,000 cm^{-1} in diethyl ether. A stretching vibration was observed at 1,680 cm^{-1} in all of the membranes regardless of the co-solvent, which was attributed to the C=C bonds. From the figures, it is clearly observed that the intensity of the typical bands of polyamide was increased by the addition of co-solvents, which specifies that the amounts of polyamide were increased by the addition of a co-solvent. Superior amounts of polyamide also look like to widen the expansion and thicken the polyamide skin layer. Moreover, the formation of a polyamide is based on the types and concentrations of co-solvents that are added, while both diethyl ether and ethyl acetate exhibited an increase in the absorbance ratio with increases in the concentrations that were added.

3.3.2. Contact angle measurements

Contact angle measurements were collected for all of the different membranes produced in this study using a droplet of DI water, which was placed on the homogeneous surfaces of the membranes prepared with different concentrations of co-solvent in the range of 0.5–5 wt%. The results of these experiments are shown in Fig. 7. The results revealed that the contact

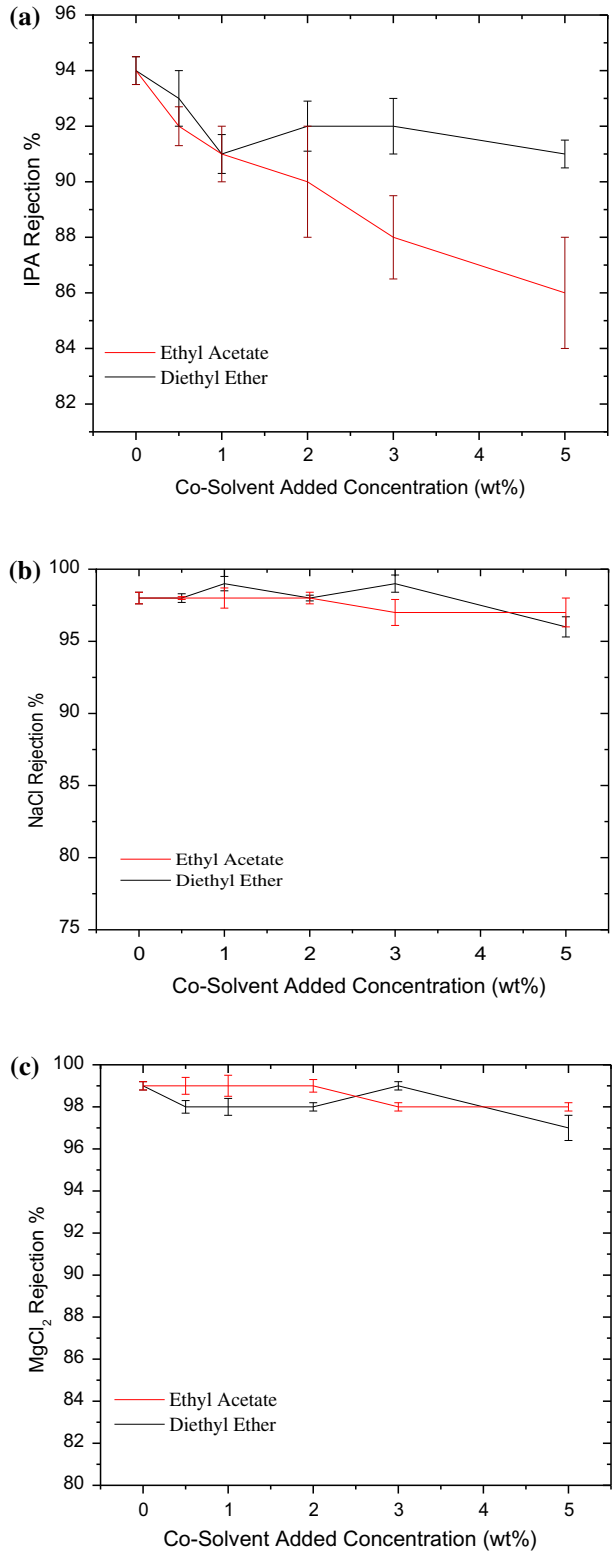

Fig. 9. Salt rejection properties of membranes containing different co-solvents: : (a) salt rejection of IPA, (b) salt rejection of NaCl, and (c) Salt rejection of MgCl2.

angle increased significantly with an increasing co-solvent concentration, and reached its maximum value for membranes containing 2 wt% diethyl ether or ethyl acetate before decreasing with further increases in the co-solvent concentration. Wettability of ethyl acetate is higher than diethyl ether, because ethyl acetate is chosen as bridging liquid, all being less soluble in water and showing good wettability. The present study displays that the bridging liquid has a significant influence on the product properties; in ethyl acetate, no agglomerates are formed and also ethyl acetate has very low interfacial tension 6.8 dyn/cm compared to diethyl ether. So, the wettability of ethyl acetate is higher than diethyl ether. Furthermore, the contact angle was found to be higher for membranes containing ethyl acetate then diethyl ether at all of the concentrations tested.

4. Membrane performance

4.1. Permeate flux

Isopropyl alcohol (IPA), NaCl, and $MgCl_2$ solutions were used to measure permeate fluxes through the different PA membranes containing different co-solvents. The results of these experiments are shown in Fig. 8(a)–(c) for IPA, NaCl, and $MgCl_2$, respectively, and it clearly show that the rate of flux generally increased with an increasing co-solvent concentration. High flux was observed in the presence of both the co-solvents tested in the PA membranes, which was attributed to the large pore sizes of these membranes. These results were also found to be in agreement with those obtained by other researchers [18,19,26,27].

4.2. Salt rejection

Fig. 9(a) shows that the salt rejection of IPA decreased with an increasing co-solvent concentration for both ethyl acetate and diethyl ether, whereas Fig. 9(b) and c shows that there was very little salt rejection of NaCl or $MgCl_2$ with either of the two co-solvents (i.e. diethyl ether and ethyl acetate).

4.3. Summary of modified RO membranes properties of previous studies

There have been numerous reports in the literature regarding the performance of commercial membranes prepared by the interfacial polymerization of TFC membranes and aromatic polyamides, as well as TFC desalination membranes prepared from MPD and TMC. The transport properties of the membranes prepared in this study were therefore compared with the properties of several similar membranes from the literature, and the details of this comparison process have been provided below in Table 2. As can be seen

Table 2
Summary of the data from previous studies

Co-solvents type	Method	Type	Modified membrane properties	NaCl salt rejection (%)	Flux L/m^2 h	Refs.
Diethyl ether and ethyl acetate	IP (MPD/TMC) In n-Heptane solvent	3 wt% diethyl ether	Flux increased Salt rejection decrease	99	42.17	[a]
		5 wt% ethyl acetate	Flux increased Salt rejection decrease	97	54.23	[a]
Acetone, diethyl ether and ethyl acetate	IP (MPD/TMC) In n-Hexane solvent	1 wt% acetone	Flux increase salt rejection decrease	99	50.1	[14]
		3 wt% ethyl acetate	Flux increased salt rejection decrease	99	75.1	
		5 wt% diethyl ether	Flux increase salt rejection decrease	99.4	50.1	
Acetone	IP (MPD/TMC) In n-Hexane solvent	2 wt% acetone	Increased pore size flux increase salt rejection decrease	99.4	1E−11 m^3/m Pa s	[15]
Acetone, diethyl ether, ethyl acetate, Toluene, Isopropyl alcohol	IP (MPD/TMC) In n-Hexane solvent	Acetone ethyl acetate	Flux increase Flux increase	98 99.5	41.74 45.9	[19]

[a]Current Study.

from Table 2, the RO performance of the resulting membrane is enhanced effectively by adopting the co-solvent-assisted interfacial polymerization method in the manufacturing process of the polyamide membrane. The water flux of the TFC membrane increases from about 42.17 l/m^2 h for 3 wt% diethyl ether and as high 54.23 l/m^2 h for 5 wt% ethyl acetate, while the salt rejection ascends simultaneously from around 97% to a higher value of 99%.

5. Conclusions

Several PA thin-film composite membranes have been developed by interfacial polymerization in a non-polar heptane medium using diethyl ether or ethyl acetate as a co-solvent. SEM images showed that the membrane surfaces were smooth with an average surface roughness in the range of 25–32 nm. TGA analysis indicated that these newly developed membranes have high thermal stability. High contact angles were also observed in the PA membranes prepared using diethyl ether or ethyl acetate as a co-solvent. Notably, high fluxes and steady salt rejection properties were observed for the PA membranes produced using diethyl ether and ethyl acetate as co-solvents.

Acknowledgement

Authors are grateful to King Abdulaziz City for Science and Technology, Riyadh, Saudi Arabia, for financially supporting this work and providing the use of the facilities in its labs.

References

[1] G.D. Jenerette, L. Larsen, A global perspective on changing sustainable urban water supplies, Global Planet. Change 50 (2006) 202–211.
[2] I.C. Kim, K.H. Lee, Dyeing process wastewater treatment using fouling resistant nanofiltration and reverse osmosis membranes, Desalination 192 (2006) 246–251.
[3] H. Ju, B.D. McCloskey, A.C. Sagle, Y.H. Wu, V.A. Kusuma, B.D. Freeman, Crosslinked poly(ethylene oxide) fouling resistant coating materials for oil/water separation, J. Membr. Sci. 307 (2008) 260–267.
[4] X.S. Peng, J. Jin, Y. Nakamura, T. Ohno, L. Ichinose, Ultrafast permeation of water through protein-based membranes, Nat. Nanotechnol. 4 (2009) 353.
[5] R.W. Baker, Membrane Technology and Applications, second ed., John Wiley & Sons Ltd, England, 2004.
[6] M. Kurihara, M. Hanakawa, Megaton water system: Japanese national research and development project on seawater desalination and waste water reclamation, Desalination 308 (2013) 131–137.
[7] W. Xie, G.M. Geise, B.D. Freeman, H.S. Lee, G. Byun, J.E. McGrath, Polyamide interfacial composite membranes prepared from m-phenylene diamine, trimesoyl chloride and a new disulfonated diamine, J. Membr. Sci. 403–404 (2012) 152–161.
[8] D.J. Mohan, L. Kullová, A Study on the relationship between preparation condition and properties/performance of polyamide TFC membrane by IR, DSC, TGA, and SEM techniques, Desalin. Water Treat. 51 (2012) 586–596.
[9] S.Y. Park, S.G. Kim, J.H. Chun, B.H. Chun, S.H. Kim, Fabrication and characterization of the chlorine-tolerant disulfonated poly(arylene ether sulfone)/hyperbranched aromatic polyamide-grafted silica composite reverse osmosis membrane, Desalin. Water Treat. 43 (2012) 221–229.
[10] H. Dong, X.Y. Qu, L. Zhang, L.H. Cheng, H.L. Chen, C.J. Gao, Preparation and characterization of surface-modified zeolite-polyamide thin film nanocomposite membranes for desalination, Desalin. Water Treat. 34 (2011) 6–12.
[11] M.M. Said, A.M. El-Aassar, Y.H. Kotp, H.A. Shawky, M.S.A. Abdel Mottaleb, Performance assessment of prepared polyamide thin film composite membrane for desalination of saline groundwater at Mersa Alam-Ras Banas, Red Sea Coast, Egypt, Desalin. Water Treat. 51 (2013) 4927–4937.
[12] R.J. Petersen, Composite reverse osmosis and nanofiltration membranes, J. Membr. Sci. 83 (1993) 81–150.
[13] J.E. Cadotte, Interfacially synthesized reverse osmosis membrane, U.S. Patent 4,277,344, 1981.
[14] T. Kamada, T. Ohara, T. Shintani, T. Tsuru, Optimizing the preparation of multi-layered polyamide membrane via the addion of a co-solvent, J. Membr. Sci. 453 (2014) 489–497.
[15] C. Kong, T. Shintani, T. Kamada, V. Freger, T. Tsuru, Co-solvent mediated synthesis of thin polyamide membrane, J. Membr. Sci. 384 (2011) 10–16.
[16] C. Kong, M. Kenezashi, T. Yamomoto, T. Shintani, T. Tsuru, Controlled synthesis of high performance polyamide membrane with thin dense layer for water desalination, J. Membr. Sci. 362 (2010) 76–80.
[17] B.H. Jeong, E.M.V. Hoeka, Y. Yan, A. Subramani, Interfacial polymerization of thin film nanocomposites: A new concept for reverse osmosis membranes, J. Membr. Sci. 294 (2007) 1–7.
[18] C. Kong, T. Shintani, T. Kamad, V. Freger, T. Tsur, Co-solvent-mediated synthesis of thin polyamide membranes, J. Membr. Sci. 384 (2011) 10–1.
[19] T. Kamada, T. Ohara, T. Shintani, T. Tsuru, Controlled surface morphology of polyamide membranes via the addition of co-solvent for improved permeate flux, J. Membr. Sci. 467 (2014) 303–312.
[20] S. Yua, M. Liua, X. Liua, C. Gao, Performance enhancement in interfacially synthesized thin-film composite polyamide-urethane reverse osmosis membrane for seawater desalination, J. Membr. Sci. 342 (2009) 313–320.
[21] H. Zou, Y. Jin, J. Yang, H. Dai, X. Yu, J. Xu, Synthesis and characterization of thin film composite reverse osmosis membranes via novel interfacial polymerization approach, Sep. Purif. Technol. 72 (2010) 256–262.

[22] M.L. Lind, D.E. Suk, T.V. Nguyen, E.M.V. Hoek, Tailoring the structure of thin film nanocomposite membranes to achieve seawater RO membrane performance, Environ. Sci. Technol. 44 (2010) 8230–8235.
[23] S. Yu, X. Liu, J. Liu, D. Wu, M. Liu, C. Gao, Surface modification of thin-film composite polyamide reverse osmosis membranes with thermo-responsive polymer (TRP) for improved fouling resistance and cleaning efficiency, Sep. Purif. Technol. 76 (2011) 283–291.
[24] R. Guan, H. Zou, D. Lu, C. Gong, Y. Liu, Polyethersulfone sulfonated by chlorosulfonic acid and its membrane characteristics, Eur. Polym. J. 41 (2005) 1554–1560.
[25] J. Zuo, T.S. Chung, Design and synthesis of a fluoro-silane amine monomer for novel thin film composite membranes to dehydrate ethanol via pervaporation, J. Mater. Chem. 1 (2013) 9814–9826.
[26] G. Cornelis, K. Boussu, B. Van der Bruggen, I. Devreese, C. Vandecasteele, Nanofiltration of nonionic surfactants: Effect of the molecular weight cutoff and contact angle on flux behavior, Ind. Eng. Chem. Res. 44 (2005) 7652–7658.
[27] N.M. Mokhtar, W.J. Lau, P.S. Goh, Effect of hydrophobicity degree on PVDF hollow fiber membranes for textile wastewater treatment using direct contact membrane distillation, Jurnal Teknologi (Sciences & Engineering), 65 (2013) 77–81.